



Published in final edited form as:

Biochem J. 2015 May 1; 467(3): 517–527. doi:10.1042/BJ20131635.

Bioenergetic programming of macrophages by the apolipoprotein A-I mimetic peptide 4F

Geeta Datta^{*,†,1}, Philip A. Kramer^{‡,1}, Michelle S. Johnson[‡], Hirotaka Sawada[‡], Lesley E. Smythies^{*}, David K. Crossman[§], Balu Chacko^{†,‡}, Scott W. Ballinger^{†,‡}, David G. Westbrook[‡], Palgunachari Mayakonda^{*}, G. M. Anantharamaiah^{*,§,2}, Victor M. Darley-Usmar^{†,‡}, and C. Roger White^{*,†,3}

^{*}Department of Medicine, University of Alabama at Birmingham, Birmingham, AL 35294, U.S.A

[†]Center for Free Radical Biology, University of Alabama at Birmingham, Birmingham, AL 35294, U.S.A

[‡]Department of Pathology, University of Alabama at Birmingham, Birmingham, AL 35294, U.S.A

[§]Department of Biochemistry and Molecular Genetics, University of Alabama at Birmingham, Birmingham, AL 35294, U.S.A

Abstract

The apoA-I (apolipoprotein A-I) mimetic peptide 4F favours the differentiation of human monocytes to an alternatively activated M2 phenotype. The goal of the present study was to test whether the 4F-mediated differentiation of MDMs (monocyte-derived macrophages) requires the induction of an oxidative metabolic programme. 4F treatment induced several genes in MDMs that play an important role in lipid metabolism, including PPAR γ (peroxisome-proliferator-activated receptor γ) and CD36. Addition of 4F was associated with a significant increase in FA (fatty acid) uptake and oxidation compared with vehicle treatment. Mitochondrial respiration was assessed by measurement of the OCR (oxygen-consumption rate). 4F increased basal and ATP-linked OCR as well as maximal uncoupled mitochondrial respiration. These changes were associated with a significant increase in Ψ_m (mitochondrial membrane potential). The increase in metabolic activity in 4F-treated MDMs was attenuated by etomoxir, an inhibitor of mitochondrial FA uptake. Finally, addition of the PPAR γ antagonist T0070907 to 4F-treated MDMs reduced the expression of CD163 and CD36, cell-surface markers for M2 macrophages, and reduced basal and ATP-linked OCR. These results support our hypothesis that the 4F-mediated differentiation of

© The Authors Journal compilation

³To whom correspondence should be addressed (crwhite@uab.edu).

¹These authors made an equal contribution to this work.

²G.M. Anantharamaiah is a Principal in Bruin Pharma, Inc.

AUTHOR CONTRIBUTION

Geeta Datta and Roger White designed the experiments, analysed data, interpreted results and wrote and revised the paper. Geeta Datta also carried out mitochondrial membrane potential measurements. Philip Kramer and Balu Chacko conducted Seahorse experiments and analysed the data. Michelle Johnson and Hirotaka Sawada performed Western blot analyses and qRT-PCR studies. Lesley Smythies conducted flow cytometry experiments and analysed data. David Crossman carried out transcriptional profiling data analysis. Scott Ballinger and David Westbrook carried out mitochondrial copy number experiments and data analysis. Palgunachari Mayakonda synthesized the peptide used in these studies. Anantharamaiah provided peptide and helped with the revision of the paper. Victor Darley-Usmar designed mitochondrial experiments, analysed data and helped with the revision of the paper.

MDMs to an anti-inflammatory phenotype is due, in part, to an increase in FA uptake and mitochondrial oxidative metabolism.

Keywords

apoA-I mimetic peptide; fatty acid oxidation; macrophage polarization; mitochondrial respiration; oxygen consumption rate; PPAR γ

INTRODUCTION

Classically activated M1 and alternatively activated M2 macrophages exert opposing effects with respect to inflammation and possess different metabolic profiles [1]. Glycolytic activity is enhanced in M1 macrophages due to the increased requirement for the rapid generation of ATP for cellular processes such as respiratory burst activity [2]. In contrast, an increase in oxidative phosphorylation in M2 macrophages is thought to facilitate secretion of proteins that facilitate wound repair and healing, processes that require the sustained, but not necessarily rapid, generation of ATP [3,4]. Furthermore, treatment of tissue-resident macrophages with rotenone or 3-nitropropionic acid, inhibitors of oxidative phosphorylation, prevented the alternative activation of M2 macrophages, as revealed by a reduction in arginase expression and up-regulation of pro-inflammatory cytokines [1].

PPAR γ (peroxisome-proliferator-activated receptor γ), PGC-1 (PPAR γ co-activator 1) isoforms and LXR α (liver X receptor α) are thought to play critical roles in M2 macrophage differentiation via stimulatory effects on lipid metabolism and mitochondrial respiration [1,5]. LXR α and PPARs protect the cell from cholesterol overload by inducing ABCA1 (ATP-binding cassette transporter A1) expression and suppress M1 macrophage activation by down-regulating nitric oxide synthase 2, IL (interleukin)-6, cyclo-oxygenase 2 and components of the NF- κ B (nuclear factor κ B) pathway [1,6–8]. Activation of LPL (lipoprotein lipase) by LXR α provides FAs (fatty acids) that act as ligands for PPAR γ [9]. Activation of PPAR γ results in the up-regulation of the scavenger receptor CD36 and the mannose receptor MRC1 (or CD206), signature genes of antiinflammatory M2 macrophages [10,11]. ATP formation in M2 macrophages is increased as these cells switch from glycolysis to FA oxidation for energy production. PPARs have been shown to stimulate oxidative phosphorylation and mitochondrial biogenesis (formation of new mitochondria) during the alternative activation of M2 macrophages [12]. As a result, mitochondrial oxygen consumption is significantly increased in M2 compared with M1 macrophages [13]. Taken together, these data demonstrate that the modulation of cellular bioenergetic function is potentially an important strategy for controlling macrophage differentiation and function and a viable therapeutic target.

The apoA-I (apolipoprotein A-I) mimetic peptide 4F mimics properties of apoA-I including the ability to mediate cholesterol efflux and inhibit monocyte chemotaxis [14]. 4F is an 18-residue peptide, possesses an amphipathic helical structure and, in the presence of lipid, forms discoidal HDL (high-density lipoprotein)-like particles. Previous studies show that the peptide exerts vasoprotective effects under acute (sepsis) and chronic (atherosclerosis, diabetes, lupus) inflammatory conditions [15]. Our previous observation that 4F, similar to

apoA-I, induces the differentiation of monocytes to an alternatively activated M2 macrophage phenotype provides a potential mechanism to explain the anti-inflammatory effect of the peptide [16,17]. In the present study, we tested the hypothesis that the effects of 4F on macrophage phenotype and function are associated with a change in cellular bioenergetics. We show that 4F treatment of MDMs increases the expression of proteins that regulate cellular lipid metabolism and mitochondrial oxidative metabolism. These changes are accompanied by an increase in FA uptake/metabolism and mitochondrial respiration.

EXPERIMENTAL

Peptide synthesis

The apoA-I mimetic 4F, an 18-residue class A amphipathic helical peptide with the sequence Ac-DWFKAFYDKVAEKFKEAF-NH₂, was synthesized using the solid-phase peptide synthesis method [18].

Cell culture

Human subject protocols were approved by the Institutional Review Board of the University of Alabama at Birmingham. Primary human PBMCs (peripheral blood mononuclear cells) were isolated from buffy coats obtained from Research Blood Components by Ficoll gradient separation. Monocyte cultures were derived by adherence as described previously [16,17]. In some studies, monocytes were enriched using CD14-labelled beads and magnetic separation before culture. Monocytes were grown in RPMI 1640 medium containing 10% (v/v) FBS over a 7-day period. Over this period, monocytes attach to the cell culture substrate and adopt a macrophage phenotype. 4F (50 µg/ml) or an equivalent volume of saline vehicle was added to cells upon seeding and replenished on days 3 and 5. MDMs were harvested for study on day 7. In some experiments, the PPAR γ antagonist T0070907 (10 µM; Cayman Chemical Co.) was added to the incubation medium for the final 24 h of the incubation period.

Microarray

Total RNA was isolated from MDMs, and purity was assessed by gel electrophoresis (Agilent 2100 Bioanalyzer). Transcriptional profiling experiments were then carried out using the Affymetrix Human Gene ST 1.0 Array, as described previously [17]. Data were analysed using GeneSpring GX software. Differences between treatment groups were determined by one-way ANOVA and the multiple testing correction method of Benjamini Hochberg. A corrected *P*-value (*q*-value) was then calculated to correct for false-positive discoveries. Datasets were deposited in the NCBI's Gene Expression Omnibus repository (GEO submission #GSE36933) [17].

qRT-PCR (quantitative real-time PCR)

cDNA was synthesized from purified RNA in a reaction mixture containing oligo(dT)₂₀ primer and SuperScript III reverse transcriptase according to the manufacturer's instructions (Invitrogen). Gene-specific primer pairs were obtained from the NIH qPrimerDepot and were validated using PubMed Gene and Sequence Manipulation Suite (Table 1). qRT-PCR

was performed on the ABI 7300 Real-Time PCR System using SYBR Green PCR Master Mix (Invitrogen). *RPL37A* was used as the housekeeping gene.

Immunoblotting

Cell lysates (30 μ g) of MDMs were subjected to SDS/PAGE, transferred on to nitrocellulose membranes and probed for different proteins using specific primary antibodies against PPAR γ , CD36 and β -actin (Santa Cruz Biotechnology), VDAC1 (voltage-dependent anion channel 1) and SDHB (succinate dehydrogenase subunit B; Abcam), and cytochrome *c* oxidase 1 (Invitrogen). Antibodies against aconitase were provided by Dr. Scott Ballinger. After labelling with appropriate secondary antibodies, proteins were visualized using SuperSignal West Dura Extended Duration substrate (Life Technologies) using the FluorChem M Western blot imaging system (ProteinSimple). Image analysis and densitometry was performed using AlphaView SA software (ProteinSimple). Quantification was only performed on images in which band intensities were below the saturation threshold, as set by the imaging system. Ponceau S staining was performed on all membranes after transfer to ensure transfer efficiency and equal protein loading (results not shown). β -Actin was also used as loading template. Proteins that migrated near the same molecular mass had duplicate membranes probed.

Flow cytometry

Day 7 MDMs (2×10^5 cells) were phenotyped using optimal concentrations of antibodies against M2 macrophage surface markers, CD163-PE (phycoerythrin) and CD36-FITC or control PE- and FITC-labelled irrelevant isotype control antibodies (BD Biosciences). MDMs were incubated with antibodies in the dark for 20 min at 4°C using our standard protocols [19], washed with 2 ml of PBS, fixed with 1 % (w/v) paraformaldehyde cytofix (BD Biosciences) and analysed by flow cytometry. FACS data were analysed with FlowJo software (Tree Star).

Measurement of FA uptake and oxidation

Vehicle- and 4F-treated MDMs were incubated with FA-free BSA-conjugated [14 C]oleic acid. At different intervals, cells were washed extensively and lysed. The incorporated radioactivity was then measured using a scintillation counter. FA oxidation in MDMs was monitored as described previously [20]. Briefly, cells were incubated with [14 C]oleic acid for 2h at 37°C. At the end of the incubation period, 1 M perchloric acid was added to the conditioned medium to precipitate unoxidized FAs. 14 CO $_2$ liberated by the oxidation of oleic acid was then trapped on a filter disc saturated with 1 M sodium hydroxide and counted using a scintillation counter. Radiolabelled FA uptake and oxidation were normalized to cellular protein content.

Measurement of mitochondrial function in MDMs using extracellular flux analysis

OCRs (oxygen-consumption rates) in intact MDMs were determined using an Extracellular Flux Analyzer (XF96) from Seahorse Bioscience. At 24 h before bioenergetics assessment, MDMs were transferred on to XF microplates at an optimum seeding density of 150000 cells/well in RPMI 1640 medium containing 10 % (v/v) FBS without Phenol Red. Cells

were washed with minimally buffered Dulbecco's modified Eagle's medium (pH 7.4) and allowed to equilibrate for 1 h before measuring OCR, as described previously [21,22]. Several indices of mitochondrial function were measured in MDMs by sequential addition of oligomycin (1 μ g/ml), FCCP (carbonyl cyanide *p*-trifluoromethoxyphenylhydrazone; 0.9 μ M) and antimycin A (10 μ M), as described previously [21]. These included: (i) basal oxygen consumption, (ii) ATP-linked oxygen consumption, (iii) maximal respiratory capacity, (iv) reserve capacity, and (v) non-mitochondrial oxygen consumption. In some experiments, the effects of FA uptake on mitochondrial OCR was assessed in the presence and absence of etomoxir (50 μ M), a CPT1 (carnitine palmitoyltransferase 1) inhibitor. In other experiments, effects of the PPAR γ antagonist T0070907 (10 μ M) on the OCR were tested.

Measurement of Ψ_m

Vehicle- and 4F-treated MDMs were incubated with TMRM (tetramethylrhodamine methyl ester; 100 nM) for 30 min at 37°C, and TMRM fluorescence was read using a plate reader with excitation at 548 nm and emission at 573 nm. In control experiments, cells were treated with the mitochondrial uncoupling agent FCCP (10 μ M) before measurement of fluorescence in order to disrupt the proton electrochemical gradient and Ψ_m (mitochondrial membrane potential).

Mitochondrial copy number

DNA was extracted from MDMs (Qiagen kit), followed by quantification using an Invitrogen PicoGreen Quant-iT™ kit. Samples were then diluted to a final concentration of 3 ng/ μ l. Mitochondrial DNA copy number was determined by performing a human mitochondrial short PCR, as described previously [23]. Then, 15 ng of total genomic DNA per reaction was used for qPCR. Duplicate samples underwent PCR amplification and were resolved on a 10% polyacrylamide gel. The dried gel was placed on a phosphor-screen, and an image was acquired after 12 h on a Storm PhosphorImager scanner (Molecular Dynamics). DNA product bands were quantified using image analysis software (ImageQuant) and compared with untreated controls. Mitochondrial copy number was normalized to the total amount of DNA per sample.

RESULTS

4F transcriptionally regulates genes that influence lipid metabolism

Our previous studies showed that depletion of cellular cholesterol in 4F-treated MDMs was associated with the differentiation of these cells to an anti-inflammatory M2 phenotype [16,17]. We predicted that a reduction in cell cholesterol would lead to underlying changes in the expression of genes that regulate lipid metabolism. In the present study, transcriptional analyses of vehicle- and 4F-treated MDMs were performed, revealing changes in key proteins involved in lipid metabolism (Table 2). Expression of LXR α and PPAR γ were significantly increased in 4F-treated MDMs compared with vehicle control. LXR α is an important transcriptional regulator of LPL which hydrolyses triacylglycerol-rich lipoproteins, resulting in the release of free FAs. PPAR γ regulates FA metabolism by inducing the expression of CD36, a membrane receptor for FAs and lipoproteins. 4F also

up-regulated *PPARGC1B*, the gene for PGC-1 β , which is known to interact with PPAR γ to increase mitochondrial respiration and cell differentiation [1]. Finally, 4F increased expression of FABPs (fatty-acid-binding proteins) 4 and 5, which act as lipid chaperones in the cell, and up-regulated VDAC1, a regulator of mitochondrial solute transport [24]. VDAC1 also interacts with CPT1a to form a complex that facilitates mitochondrial FA uptake and oxidation [25,26]. qRT-PCR experiments were performed in order to validate several genes in the microarray. Gene-specific primer sequences are shown in Table 1. Similar to the microarray data, 4F significantly increased mRNA expression for PPAR γ , FABP4, FABP5 and VDAC1 (Table 3). There was a trend towards increased mRNA expression for LPL and CD36 in 4F-treated MDMs; however, these changes were not significantly different from vehicle treatment (Table 3). No difference in *PPARGC1B* mRNA was observed.

4F increases FA uptake and β -oxidation in MDMs

Results of transcriptional studies suggested that 4F may influence macrophage phenotype/function by a mechanism involving PPAR γ up-regulation and an increase in FA uptake and metabolism. Immunoblotting studies confirmed the up-regulation of PPAR γ protein levels in 4F-treated MDMs (Figure 1). Although qRT-PCR studies did not support the increased expression of CD36 observed in the microarray, we found that 4F increased CD36 protein expression (Figure 1). Previous studies have identified PPAR γ as a critical mediator of M2 macrophage differentiation [1,5]. Our flow cytometry studies show that 4F increases the expression of CD163 and CD36, cellular markers for alternatively activated M2 macrophages, by 50% compared with vehicle treatment (Figure 2). This response was inhibited by addition of the PPAR γ antagonist T0070907 (10 μ M) to 4F-treated cells, consistent with the hypothesis that PPAR γ plays a role in 4F-mediated differentiation of macrophages to an M2 phenotype (Figure 2). In subsequent experiments, we tested whether the transcriptional up-regulation of CD36 was associated with an increase in FA uptake in 4F-treated MDMs. 4F treatment significantly increased the uptake of [14 C]oleic acid in MDMs in a time-dependent manner compared with vehicle treatment (Figure 3A). At the 4 h time point, FA uptake was increased approximately 2.5-fold by 4F treatment compared with vehicle control. Furthermore, mitochondrial FA oxidation, monitored via the liberation of radiolabelled CO $_2$, was increased approximately 2-fold by 4F treatment (Figure 3B). These data suggested that 4F increases the availability of substrates for mitochondrial respiration and oxidative phosphorylation.

The 4F-mediated increase in mitochondrial respiration is linked to up-regulation of respiratory chain proteins

To test the effects of 4F on cellular respiration in MDMs, we monitored mitochondrial respiration using a Seahorse XF96 Metabolic Flux Analyzer. Representative Seahorse profiles for MDMs treated with vehicle or 4F are depicted in Figure 4(A). Basal OCR was measured first, followed by addition of oligomycin, an inhibitor of the ATP synthase (Complex V). The difference between the basal rate and the oligomycin-insensitive rate reflects the amount of OCR that is used for ATP generation. The change in OCR after addition of FCCP yields the maximum oxygen consumption that can take place at cytochrome *c* oxidase (Complex IV). Finally, antimycin A was injected to inhibit electron

flux through Complex III. This yields the OCR that is due to non-mitochondrial sources of oxygen consumption. Bioenergetic profiles revealed that 4F treatment increased: (i) basal OCR; (ii) ATP-linked OCR; and (iii) maximum oxygen consumption (Figures 4B–4D). Absolute OCR values varied between wells and, under basal conditions, ranged from 7.02 to 8.47 and 10.56 to 11.75 pmol/min per 10^4 cells in control and 4F-treated MDMs respectively. These studies also showed that PPAR γ activation is required for the 4F-mediated increase in basal and ATP-linked OCR since these responses were abolished by pre-treatment with the antagonist T0070907 (Figures 4B and 4C).

Transcriptional analyses showed that 4F treatment resulted in an increase in expression of a number of mitochondrial genes (Table 4). These included genes encoding metabolic regulators such as aconitase 1 and 2, acyl-CoA dehydrogenase (*ACADM*), and *VDAC1*. Subunits of respiratory complexes were also up-regulated, including succinate dehydrogenase (ubiquinone) iron–sulfur subunit (Complex II) and cytochrome *c* oxidase I (Complex IV) (Table 4). Immunoblotting studies confirmed that 4F significantly increased protein expression for aconitase (type 1 and 2 isoforms), *VDAC1*, succinate dehydrogenase (ubiquinone) iron–sulfur subunit and cytochrome *c* oxidase I (Figures 5A–5D). An increase in the oxidation of respiratory chain substrates is linked to proton pumping across the inner mitochondrial membrane which gives rise to the Ψ_m [27]. The subsequent transport of protons through the ATP synthase (Complex V) is linked to the formation of ATP. In order to determine whether the 4F-mediated increase in the OCR influenced the Ψ_m , relative changes in membrane potential were measured using the fluorescent probe TMRM. 4F treatment increased TMRM-dependent fluorescence compared with vehicle, consistent with an increase in Ψ_m (Figure 5E). To determine whether the observed increases in mitochondrial gene expression and the OCR in 4F-treated MDMs was due to mitochondrial biogenesis, mitochondrial DNA copy number was measured. DNA copy number was similar in control and 4F-treated MDMs (Figure 5F).

Inhibition of FA uptake attenuates effects of 4F on mitochondrial respiration

Our data suggested that an increase in PPAR γ and CD36 expression is associated with an increase in FA uptake in 4F-treated MDMs. In order to determine whether the increase in mitochondrial OCR in 4F-treated MDMs was directly related to enhanced FA uptake, we monitored effects of the FA uptake inhibitor etomoxir on mitochondrial respiration. Bioenergetic profiles for vehicle- and 4F-treated MDMs exposed to etomoxir are shown in Figure 6. Similar to data presented in Figure 4, basal OCR was increased in 4F-treated MDMs compared with control. Addition of etomoxir reduced basal OCR in vehicle-treated MDMs by 15%. A larger decrease in basal OCR (24% reduction; $P < 0.001$) was induced by etomoxir in 4F-treated cells. As a result, a new equilibrium was established at which basal and ATP-linked OCR were similar in both vehicle- and 4F-treated MDMs. Despite this prominent inhibitory effect of etomoxir on basal and ATP-linked OCR, maximal oxygen consumption remained elevated in 4F-treated MDMs compared with vehicle treatment.

DISCUSSION

Circulating mononuclear cells infiltrate tissues, including the blood vessel wall, where they differentiate into macrophages. The differentiation pathway of monocytes is influenced by the local micro-environment [28]. In the presence of Th1 cytokines (interferon γ , IL-2) and lipopolysaccharide, monocytes differentiate into classically activated M1 macrophages [28]. These cells induce cytokine/chemokine release (tumour necrosis factor α , IL-6, monocyte chemoattractant protein 1), increase nitric oxide production via up-regulation of nitric oxide synthase 2 and play an important role in the host defence response. In contrast, Th2 cytokines (IL-4, IL-13) induce the differentiation of monocytes to an alternatively activated M2 phenotype. M2 macrophages secrete the anti-inflammatory cytokine IL-10 and play a critical role in resolving inflammation and promoting wound healing [28]. M1 and M2 macrophages possess distinct bioenergetic profiles [1]. Pro-inflammatory M1 macrophages utilize glycolysis for the rapid generation of ATP. In contrast, metabolism in M2 macrophages is characterized by an increase in β -oxidation and oxidative phosphorylation [1]. Under these conditions, M2 macrophages function to promote wound healing and repair, processes that require the prolonged generation of ATP [3,4,13].

4F is an apoA-I mimetic peptide that mimics the functional properties of HDL [29]. A recent study suggests that functional HDL induces an anti-inflammatory phenotype in macrophages by up-regulating ATF3 (activating transcription factor 3) [30]. Although the mechanism by which HDL induces the transcription factor was not described, the authors demonstrated that ATF3 acted as a repressor of NF- κ B-dependent target genes [30]. Similarly, endotoxin tolerance is associated with the adoption of an anti-inflammatory M2 phenotype in macrophages and requires the induction of ATF3 [31]. We reported previously that 4F, similar to apoA-I, induces human MDMs to adopt an M2 phenotype [16,17]. 4F-treated MDMs displayed an anti-inflammatory gene profile, expressed typical M2 macrophage surface markers and exhibited attenuated responses to lipopolysaccharide stimulation [16,17]. Under these conditions, M2 differentiation was associated with the depletion of cellular cholesterol and disruption of lipid rafts [17]. Since rafts are cholesterol-enriched microdomains that regulate a variety of cellular responses [32], we set out to determine whether 4F-induced alternative macrophage differentiation was associated with changes in cellular lipid metabolism and bioenergetics.

Gene profiling studies showed that 4F treatment up-regulated a number of genes in MDMs that play an important role in lipid metabolism and mitochondrial respiration. Specifically, microarray data showed that expression of PPAR γ , LXR α , LPL, FABP4 and FABP5 was significantly increased. The up-regulation of PPAR γ , FABP4 and FABP5 was confirmed further by qRT-PCR. PPARs and LXRs modulate cellular cholesterol content via regulation of ATP-binding cassette transporters (ABCA1, ABCG1), apoE (apolipoprotein E) and scavenger receptor class B1 [33]. LXR α also induces expression of LPL which hydrolyses triacylglycerol-rich lipoproteins, resulting in the release of free FAs that act as ligands for PPAR γ activation [9]. In the present study, *LPL* mRNA expression was increased by 4F treatment; however, this did not reach significance compared with vehicle treatment (Table 3). Both FABP4 and FABP5 were significantly up-regulated by 4F (Table 3). FABPs bind long-chain FAs and peroxisome proliferators and traffic them between cellular

compartments [24]. It follows that binding of FABP4 to PPAR γ results in an increase in its transcriptional activity [34]. PPAR γ regulates numerous genes that modulate cellular differentiation, insulin sensitivity, oxidative phosphorylation and inflammation [10]. It also up-regulates CD36, a scavenger receptor that mediates uptake of FAs and oxLDL (oxidized low-density lipoprotein) [35]. Immunoblotting data presented in Figure 1 confirmed an increase in protein expression for both PPAR γ and CD36 in 4F-treated MDMs. Subsequent functional studies showed that 4F significantly increased FA uptake and β -oxidation (Figure 3). It follows that PPAR γ -null macrophages fail to suppress inflammatory responses and do not adopt the oxidative metabolic programme associated with an M2 phenotype [3].

Microarray and Western blot studies also showed that 4F increased expression of aconitase isoforms in MDMs (Table 4 and Figure 5A). ACO1 is a cytosolic isoform of aconitase that plays an important role in regulating cellular iron metabolism [36]. ACO2 is expressed in mitochondria and regulates cellular ATP production by providing substrates for mitochondrial respiration [36]. The β -oxidation pathway also provides substrates for the mitochondrial electron transport chain. In order to determine whether 4F-mediated changes in FA metabolism resulted in an increase in mitochondrial respiration and oxidative phosphorylation, we monitored the OCR in control and 4F-treated MDMs (Figure 4). Our data show that 4F increased basal OCR in MDMs, a response that is consistent with an increase in FA uptake/oxidation [37]. Furthermore, the 4F-mediated increase in oligomycin-sensitive OCR (ATP-linked OCR) revealed a stimulatory effect of 4F on mitochondrial ATP formation [38]. Importantly, the 4F-mediated increase in basal and ATP-linked respiration was abolished by pre-treatment with the PPAR γ antagonist T0070907, demonstrating that 4F mediates its metabolic changes through PPAR γ activation. An increase in the maximum oxygen consumption induced by the mitochondrial uncoupling agent FCCP was also observed in 4F-treated MDMs, suggesting an increase in the overall activity of respiratory chain proteins or an increase in substrate availability. The increase in maximal respiration in the PPAR γ -antagonist-treated MDMs (Figure 4D) may be due to increased substrates provided by glycolysis in the control ($P = 0.0002$) and 4F-treated ($P = 0.003$) groups, as measured by the extracellular acidification rate (results not shown). Electron transfer along the respiratory chain is associated with proton pumping across the inner mitochondrial membrane and the establishment of an electrochemical potential (Ψ_m). Indeed, our data show that an increase in OCR in 4F-treated MDMs was associated with an increase in Ψ_m (Figure 5E). Basal and ATP-linked OCR were significantly attenuated in 4F-treated MDMs by the CPT1 inhibitor etomoxir (Figure 6). This result underscores the role of enhanced FA uptake and oxidation in the 4F-mediated increase in mitochondrial respiration.

Our data show further that the increased mitochondrial respiration in 4F-treated MDMs was associated with up-regulation of several genes that play an important role in mitochondrial function (Table 4). These included *ACADM* (acyl-CoA dehydrogenase) and *ACOX1* (peroxisomal acyl-CoA oxidase 1), components of the β -oxidation pathway. *ACADM* and *ACOX1* encode enzymes that degrade medium-chain FAs and catalyse the desaturation of acyl-CoAs respectively [39,40]. VDAC1 mRNA and protein were also up-regulated (Table 3 and Figure 5B). VDAC is thought to play a major role in integrating components of mitochondrial function. Among these roles is its ability to interact with CPT1 to deliver FAs

to the mitochondrion [25]. We also observed an increase in the expression of respiratory chain subunits, including succinate dehydrogenase (ubiquinone) iron–sulfur subunit (Complex II) and cytochrome *c* oxidase I (Complex IV) (Figures 5C–5D). Since data suggest that M2 macrophage differentiation is associated with mitochondrial biogenesis, we tested whether mitochondrial DNA copy number was increased in 4F-treated MDMs [1,12]. Results of these studies did not reveal a difference in DNA copy number between control and 4F-treated MDMs (Figure 5F).

Previous studies suggest that PPAR γ activation plays a role in M2 macrophage differentiation [3,4,8,12]. Bouhlef et al. [11] showed that PPAR γ co-localizes with mannose receptor and other markers for M2 macrophages in human atherosclerotic lesions. *In vitro* studies demonstrated further that IL-4-mediated alternative macrophage activation was amplified in human monocytes treated with PPAR γ agonists. PPAR γ activation enhanced the anti-inflammatory activity of these macrophages compared with treatment with IL-4 alone [11]. The role of PPAR γ in alternative macrophage activation is supported further by the observation that macrophage-specific deletion of PPAR γ prevents the maturation of myeloid cells to an M2 phenotype and reduces the tissue content of these cells [3]. Our flow cytometry studies similarly show that addition of a PPAR γ antagonist to 4F-treated MDMs significantly reduces expression of CD163 and CD36, cell-surface markers for alternative M2 macrophages [41] (Figure 2). The PPAR γ -dependent activation of alternative M2 macrophages is dependent on an increase in FA oxidation and oxidative phosphorylation. In the present study, we found that addition of the PPAR γ antagonist T0070907 to MDMs prevented the increase in basal and ATP-linked OCR induced by 4F treatment (Figure 4). The expression of genes involved in lipid uptake/metabolism (*LPL*, *CD36*, *ACADM*, *ACADL*) are reduced in IL-4-treated PPAR γ -null macrophages, resulting in a decrease in β -oxidation [3]. Similar to our observations with 4F treatment, PPAR γ activation is associated with an increase in Complex IV and VDAC expression as well as Ψ_m [3,42].

Vats et al. [1] have characterized signalling pathways associated with M2 differentiation in IL-4-treated bone-marrow-derived macrophages. Microarray analyses revealed that the maturation of anti-inflammatory macrophages was associated with the up-regulation of genes that regulate FA metabolism and mitochondrial biogenesis [1]. Development of an anti-inflammatory phenotype was dependent on the expression of the PPAR γ co-activator PGC-1 β and its transcriptional regulator STAT6 (signal transducer and activator of transcription 6) [1]. The importance of PGC-1 β in supporting mitochondrial function is underscored by studies showing that knockout of the co-activator in mice results in a reduction in mitochondrial volume and impaired cardiac performance [43]. In contrast with previous studies, our results suggest that the increase in mitochondrial respiration in 4F-treated MDMs is not associated with the formation of new mitochondria [1,13]. Furthermore, we did not observe an increase in mRNA expression for PGC-1 β in 4F-treated cells. A possible explanation for this may be related to species differences, since mitochondrial biogenesis associated with alternative macrophage activation was observed in murine macrophages [1,13]. The experiments of the present study were performed using human MDMs which may be in a more terminally differentiated state.

Mitochondrial dysfunction is associated with a number of pro-inflammatory conditions, including sepsis and ischaemia/reperfusion injury which are characterized by the uncoupling of oxidative phosphorylation [44,45]. VDAC activity is also inhibited and is associated with impaired mitochondrial function and a reduction in Ψ_m [46]. Under these conditions, increased reactive oxygen species formation induces damage to structural components of mitochondria as well as DNA [47]. It follows that tissue oxygen utilization is severely impaired and apoptotic mechanisms are activated [26,48]. 4F has been shown to reduce macrophage activation in cell culture and animal models [16,17,49,50]. Our previous studies show that 4F induces the differentiation of human MDMs to an anti-inflammatory phenotype, a response that was associated with a reduction in cellular cholesterol content [16,17]. Cholesterol depletion is also a stimulus for up-regulation of PPAR γ , suggesting a direct mechanism linking 4F to PPAR γ expression in MDMs [51]. The subsequent activation of the transcriptional regulator PPAR γ results in an increase in FA metabolism and mitochondrial respiration. The increase in oxidative metabolism may thus allow the sustained formation of ATP required to support repair processes and wound healing. In this manner, 4F may play an important role in directing macrophage differentiation and function via changes in cellular bioenergetics.

Acknowledgments

FUNDING: These studies were supported by the National Institutes of Health [grant numbers GM082952 (to G.D./C.R.W.), HL34343 (to G.M.A.), HL103859 (to S.W.B.) and T32HL07918 (to P.A.K./V.M.D.-U.)].

References

1. Vats D, Mukundan L, Odegaard JI, Zhang L, Smith KL, Morel CR, Wagner RA, Greaves DR, Murray PJ, Chawla A. Oxidative metabolism and PGC-1 β attenuate macrophage-mediated inflammation. *Cell Metab.* 2006; 4:13–24. [PubMed: 16814729]
2. Rodriguez-Prados JC, Traves PG, Cuenca J, Rico D, Aragonés J, Martín-Sanz P, Cascante M, Bosca L. Substrate fate in activated macrophages: a comparison between innate, classic, and alternative activation. *J Immunol.* 2010; 185:605–614. [PubMed: 20498354]
3. Odegaard JI, Ricardo-Gonzalez RR, Goforth MH, Morel CR, Subramanian V, Mukundan L, Red Eagle A, Vats D, Brombacher F, Ferrante AW, Chawla A. Macrophage-specific PPAR γ controls alternative activation and improves insulin resistance. *Nature.* 2007; 447:1116–1120. [PubMed: 17515919]
4. Odegaard JI, Ricardo-Gonzalez RR, Red Eagle A, Vats D, Morel CR, Goforth MH, Subramanian V, Mukundan L, Ferrante AW, Chawla A. Alternative M2 activation of Kupffer cells by PPAR δ ameliorates obesity-induced insulin resistance. *Cell Metab.* 2008; 7:496–507. [PubMed: 18522831]
5. Bensinger SJ, Tontonoz P. Integration of metabolism and inflammation by lipid-activated nuclear receptors. *Nature.* 2008; 454:470–477. [PubMed: 18650918]
6. Im SS, Osborne TF. Liver X receptors in atherosclerosis and inflammation. *Circ Res.* 2011; 108:996–1001. [PubMed: 21493922]
7. Alleva DG, Johnson EB, Lio FM, Boehme SA, Conlon PJ, Crowe PD. Regulation of murine macrophage proinflammatory and anti-inflammatory cytokines by ligands for peroxisome proliferator-activated receptor- γ : counter-regulatory activity by IFN- γ . *J Leukoc Biol.* 2002; 71:677–685. [PubMed: 11927655]
8. Rigamonti E, Chinetti-Gbaguidi G, Staels B. Regulation of macrophage functions by PPAR- α , PPAR- γ , and LXRs in mice and men. *Arterioscler Thromb Vasc Biol.* 2008; 28:1050–1059. [PubMed: 18323516]
9. Zhang Y, Repa JJ, Gauthier K, Mangelsdorf DJ. Regulation of lipoprotein lipase by the oxysterol receptors, LXR α and LXR β . *J Biol Chem.* 2001; 276:43018–43024. [PubMed: 11562371]

10. Chawla A, Barak Y, Nagy L, Liao D, Tontonoz P, Evans RM. PPAR- γ dependent and independent effects on macrophage gene expression in lipid metabolism and inflammation. *Nat Med.* 2001; 7:48–52. [PubMed: 11135615]
11. Bouhrel MA, Derudas B, Rigamonti E, Dievart R, Brozek J, Haulon S, Zawadzki C, Jude B, Torpier G, Marx N, et al. PPAR γ activation primes human monocytes into alternative M2 macrophages with anti-inflammatory properties. *Cell Metab.* 2007; 6:137–143. [PubMed: 17681149]
12. Hock MB, Kralli A. Transcriptional control of mitochondrial biogenesis and function. *Annu Rev Physiol.* 2009; 71:177–203. [PubMed: 19575678]
13. Tavakoli S, Zamora D, Ullevig S, Asmis R. Bioenergetic profiles diverge during macrophage polarization: implications for the interpretation of ^{18}F -FDG PET imaging of atherosclerosis. *J Nucl Med.* 2013; 54:1661–1667. [PubMed: 23886729]
14. Navab M, Anantharamaiah GM, Reddy ST, Van Lenten BJ, Hough G, Wagner A, Nakamura K, Garber DW, Datta G, Segrest JP, et al. Human apolipoprotein AI and A-I mimetic peptides: potential for atherosclerosis reversal. *Curr Opin Lipidol.* 2004; 15:645–649. [PubMed: 15529023]
15. White, CR.; Anantharamaiah, GM.; Datta, G. HDL mimetic peptides: novel therapeutic strategies for the treatment of inflammatory vascular disease. In: Komoda, T., editor. *The HDL Handbook: Biological Functions and Clinical Implications.* Elsevier; Amsterdam: 2010. p. 179-197.
16. Smythies LE, White CR, Maheshwari A, Palgunachari MN, Anantharamaiah GM, Chaddha M, Kurundkar AR, Datta G. Apolipoprotein A-I mimetic 4F alters the function of human monocyte-derived macrophages. *Am J Physiol Cell Physiol.* 2010; 298:C1538–C1548. [PubMed: 20219948]
17. White CR, Smythies LE, Crossman DK, Palgunachari M, Anantharamaiah GM, Datta G. Regulation of pattern recognition receptors by the apolipoprotein A-I mimetic peptide 4F. *Arterioscler Thromb Vasc Biol.* 2012; 32:2631–2639. [PubMed: 22982462]
18. Datta G, Chaddha M, Hama S, Navab M, Fogelman AM, Garber DW, Mishra VK, Epand RM, Epand RF, Lund-Katz S, et al. Effects of increasing hydrophobicity on the physical-chemical and biological properties of a class A amphipathic helical peptide. *J Lipid Res.* 2001; 42:1096–1104. [PubMed: 11441137]
19. Smythies LE, Maheshwari A, Clements R, Eckhoff D, Novak L, Vu HL, Mosteller-Barnum LM, Sellers M, Smith PD. Mucosal IL-8 and TGF- β recruit blood monocytes: evidence for cross-talk between the lamina propria stroma and myeloid cells. *J Leukoc Biol.* 2006; 80:492–499. [PubMed: 16793909]
20. Hirschey MD, Shimazu T, Goetzman E, Jing E, Schwer B, Lombard DB, Grueter CA, Harris C, Biddinger S, Ilkayeva OR, et al. SIRT3 regulates fatty acid oxidation via reversible enzyme deacetylation. *Nature.* 2010; 464:121–125. [PubMed: 20203611]
21. Hill BG, Dranka BP, Zou L, Chatham JC, Darley-Usmar VM. Importance of the bioenergetics reserve capacity in response to cardiomyocyte stress induced by 4-hydroxynonenal. *Biochem J.* 2009; 424:99–107. [PubMed: 19740075]
22. Dranka BP, Benavides GA, Diers AR, Giordano S, Zelickson BR, Reily C, Zou L, Chatham JC, Hill BG, Zhang J, et al. Assessing bioenergetic function in response to oxidative stress by metabolic profiling. *Free Radical Biol Med.* 2011; 51:1621–1635. [PubMed: 21872656]
23. Ballinger SW, Van Houten B, Conklin CA, Jin GF, Godley BF. Hydrogen peroxide causes significant mitochondrial DNA damage in human RPE cells. *Exp Eye Res.* 1999; 68:765–772. [PubMed: 10375440]
24. Smathers RL, Petersen DR. The human fatty acid-binding protein family: evolutionary divergences and functions. *Hum Genomics.* 2011; 5:170–191. [PubMed: 21504868]
25. Lee K, Kerner J, Hoppel CL. Mitochondrial carnitine palmitoyltransferase 1a (CPT1a) is part of an outer membrane fatty acid transfer complex. *J Biol Chem.* 2011; 286:25655–25662. [PubMed: 21622568]
26. Lemasters JJ, Holmuhamedov E. Voltage-dependent anion channel (VDAC) as mitochondrial governor: thinking outside the box. *Biochim Biophys Acta.* 2006; 1762:181–190. [PubMed: 16307870]

27. Amo T, Sato S, Saiki S, Wolf AM, Toyomizu M, Gautier CA, Shen J, Ohta S, Hattori N. Mitochondrial membrane potential decrease caused by loss of PINK1 is not due to proton leak, but to respiratory chain defects. *Neurobiol Dis.* 2011; 41:111–118. [PubMed: 20817094]
28. Mosser DM, Edwards JP. Exploring the full spectrum of macrophage activation. *Nat Rev Immunol.* 2008; 8:958–969. [PubMed: 19029990]
29. White CR, Garber DW, Anantharamaiah GM. Anti-inflammatory and cholesterol-reducing properties of apolipoprotein mimetics: a review. *J Lipid Res.* 2014; 55:2007–2021. [PubMed: 25157031]
30. De Nardo D, Labzin LI, Kono H, Seki R, Schmidt SV, Beyer M, Xu D, Zimmer S, Lahrman C, Schildberg FA, et al. High-density lipoprotein mediates anti-inflammatory reprogramming of macrophages via the transcriptional regulator ATF3. *Nat Immunol.* 2014; 15:152–160. [PubMed: 24317040]
31. Lawrence T, Natoli G. Transcriptional regulation of macrophage polarization: enabling diversity with identity. *Nat Rev Immunol.* 2011; 11:750–761. [PubMed: 22025054]
32. Gaus K, Rodriguez M, Ruberu KR, Gelissen I, Sloane TM, Kritharides L, Jessup W. Domain-specific lipid distribution in macrophage plasma membranes. *J Lipid Res.* 2005; 46:1526–1538. [PubMed: 15863834]
33. Hong C, Tontonoz P. Coordination of inflammation and metabolism by PPAR and LXR nuclear receptors. *Curr Opin Genet Dev.* 2008; 18:461–467. [PubMed: 18782619]
34. Ayers SD, Nedrow KL, Gillilan RE, Noy N. Continuous nucleocytoplasmic shuttling underlies transcriptional activation of PPAR γ by FABP4. *Biochemistry.* 2007; 46:6744–6752. [PubMed: 17516629]
35. Chawla A, Barak Y, Nagy L, Liao D, Tontonoz P, Evans RM. PPAR- γ dependent and independent effects on macrophage gene expression in lipid metabolism and inflammation. *Nat Med.* 2001; 7:48–52. [PubMed: 11135615]
36. Lushchak OV, Piroddi M, Galli F, Lushchak VI. Aconitase post-translational modification as a key in linkage between Krebs cycle, iron homeostasis, redox signaling, and metabolism of reactive oxygen species. *Redox Rep.* 2014; 19:8–15. [PubMed: 24266943]
37. Newsholme P, Gordon S, Newsholme EA. Rates of utilization and fates of glucose, glutamine, pyruvate, fatty acids and ketone bodies by mouse macrophages. *Biochem J.* 1987; 242:631–636. [PubMed: 3593269]
38. Brand MD, Nicholls DG. Assessing mitochondrial dysfunction in cells. *Biochem J.* 2011; 435:297–312. [PubMed: 21726199]
39. Thorpe C, Kim JJ. Structure and mechanism of action of the acyl-CoA dehydrogenases. *FASEB J.* 1995; 9:718–725. [PubMed: 7601336]
40. Osumi T, Hashimoto T, Ui N. Purification and properties of acyl-CoA oxidase from rat liver. *J Biochem.* 1980; 87:1735–1746. [PubMed: 7400120]
41. Porcheray F, Viaud S, Rimaniol AC, Léone C, Samah B, Dereuddre-Bosquet N, Dormont D, Gras G. Macrophage activation switching: an asset for the resolution of inflammation. *Clin Exp Immunol.* 2005; 142:481–489. [PubMed: 16297160]
42. Wu JS, Lin TN, Wu KK. Rosiglitazone and PPAR- γ overexpression protect mitochondrial membrane potential and prevent apoptosis by upregulating anti-apoptotic Bcl-2 family proteins. *J Cell Physiol.* 2009; 220:58–71. [PubMed: 19229877]
43. Lelliott CJ, Medina-Gomez G, Petrovic N, Kis A, Feldmann HM, Bjursell M, Parker N, Curtis K, Campbell M, Hu P, et al. Ablation of PGC-1 β results in defective mitochondrial activity, thermogenesis, hepatic function, and cardiac performance. *PLoS Biol.* 2006; 4:e369. [PubMed: 17090215]
44. Azevedo LC. Mitochondrial dysfunction during sepsis. *Endocr Metab Immune Disord Drug Targets.* 2010; 10:214–223. [PubMed: 20509844]
45. Moon KH, Hood BL, Mukhopadhyay P, Rajesh M, Abdelmegeed MA, Kwon YI, Conrads TP, Veenstra TD, Song BJ, Pacher P. Oxidative inactivation of key mitochondrial proteins leads to dysfunction and injury in hepatic ischemia reperfusion. *Gastroenterology.* 2008; 135:1344–1357. [PubMed: 18778711]

46. Chopra M, Golden HB, Mullapudi S, Dowhan W, Dostal DE, Sharma AC. Modulation of myocardial mitochondrial mechanisms during severe polymicrobial sepsis in the rat. *PLoS ONE*. 2011; 6:e21285. [PubMed: 21712982]
47. Brealey D, Singer M. Mitochondrial dysfunction in sepsis. *Curr Infect Dis Rep*. 2003; 5:365–371. [PubMed: 13678565]
48. Fink MP. Cytopathic hypoxia: mitochondrial dysfunction as mechanism contributing to organ dysfunction in sepsis. *Crit Care Clin*. 2001; 17:219–237. [PubMed: 11219231]
49. Navab M, Anantharamaiah GM, Hama S, Hough G, Reddy ST, Frank JS, Garber DW, Handattu S, Fogelman AM. D-4F and statins synergize to render HDL antiinflammatory in mice and monkeys and cause lesion regression in old apolipoprotein E-null mice. *Arterioscler Thromb Vasc Biol*. 2005; 25:1426–1432. [PubMed: 15845909]
50. Garber DW, Datta G, Chaddha M, Palgunachari MN, Hama SY, Navab M, Fogelman AM, Segrest JP, Anantharamaiah GM. A new synthetic class A amphipathic peptide analogue protects mice from diet-induced atherosclerosis. *J Lipid Res*. 2001; 42:545–552. [PubMed: 11290826]
51. Fajas L, Schoonjans K, Gelman L, Kim JB, Najib J, Martin G, Fruchart JC, Briggs M, Spiegelman BM, Auwerx J. Regulation of peroxisome proliferator-activated receptor gamma expression by adipocyte differentiation and determination factor 1/sterol regulatory element binding protein 1: implications for adipocyte differentiation and metabolism. *Mol Cell Biol*. 1999; 19:5495–5503. [PubMed: 10409739]

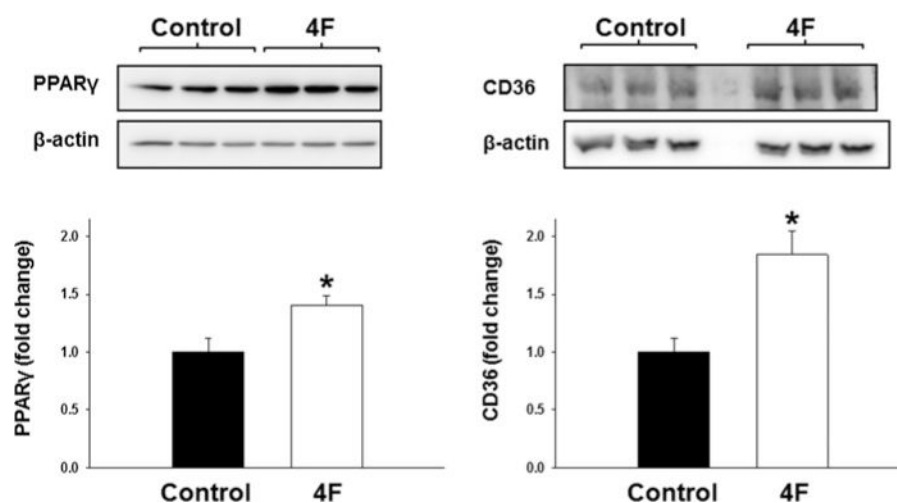


Figure 1. 4F treatment up-regulates the expression of PPAR γ and CD36 in MDMs
The protein expression for PPAR γ or CD36 was measured by densitometry in control (black bar) and 4F-treated (white bar) MDMs. Results are mean \pm S.E.M. fold changes in protein expression compared with control treatment ($n = 3-6$). * $P < 0.05$ compared with control.

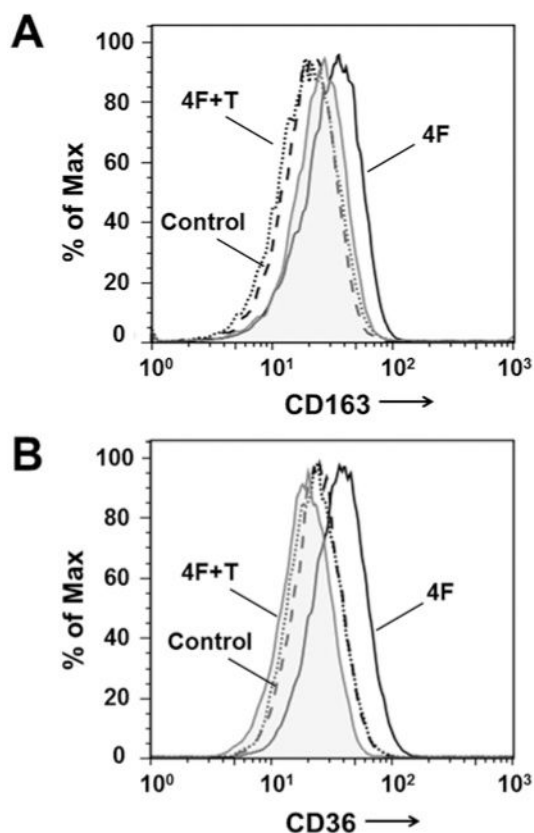


Figure 2. Inhibition of PPAR γ prevents the 4F-mediated up-regulation of M2 macrophage markers

Vehicle or the PPAR γ antagonist T0070907 (10 μ M) was added to 4F-treated MDMs for 24 h before isolation. Cells were stained with antibodies against the M2 macrophage markers CD163 or CD36 and monitored by flow cytometry. 4F significantly increased expression of CD163 (**A**) and CD36 (**B**) in MDMs in a manner that was inhibited by T0070907. Representative histograms for each marker are shown for MDMs treated with vehicle (---), 4F (—) or 4F followed by addition of T0070907 (...). The shaded histogram represents the isotype control.

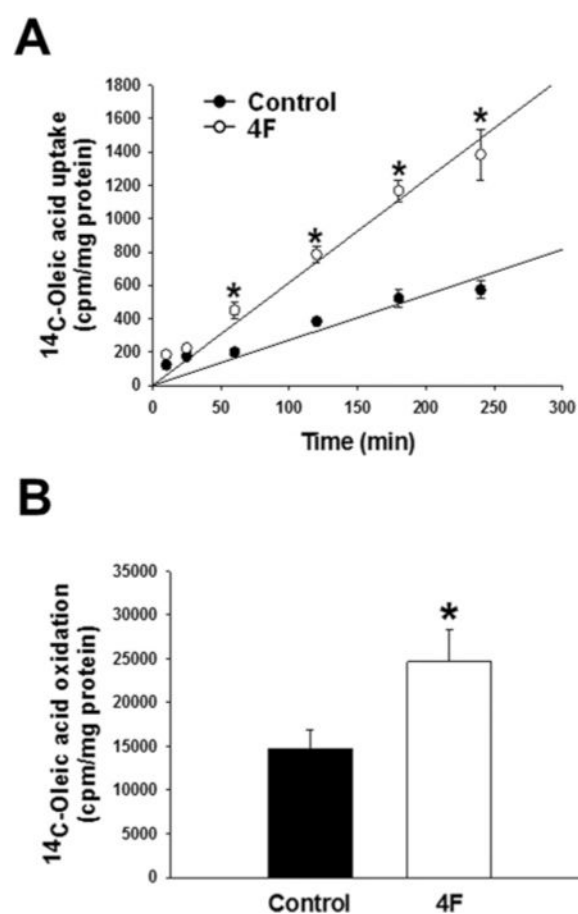


Figure 3. 4F increases FA uptake and oxidation in MDMs

[¹⁴C]oleic acid was added to control and 4F-treated MDMs for periods of up to 4 h. Cells were collected at the indicated time points and lysed, and incorporated radioactive counts were measured (A). Control and 4F-treated MDMs were incubated with [¹⁴C]oleic acid for 2 h at 37°C. ¹⁴CO₂ liberated by the complete oxidation of oleic acid was trapped on a filter disc and counted using a scintillation counter (B). In each experiment, radioactive counts were normalized to cell protein content. Results are means ± S.E.M. (*n* = 3). **P* < 0.05 compared with control.

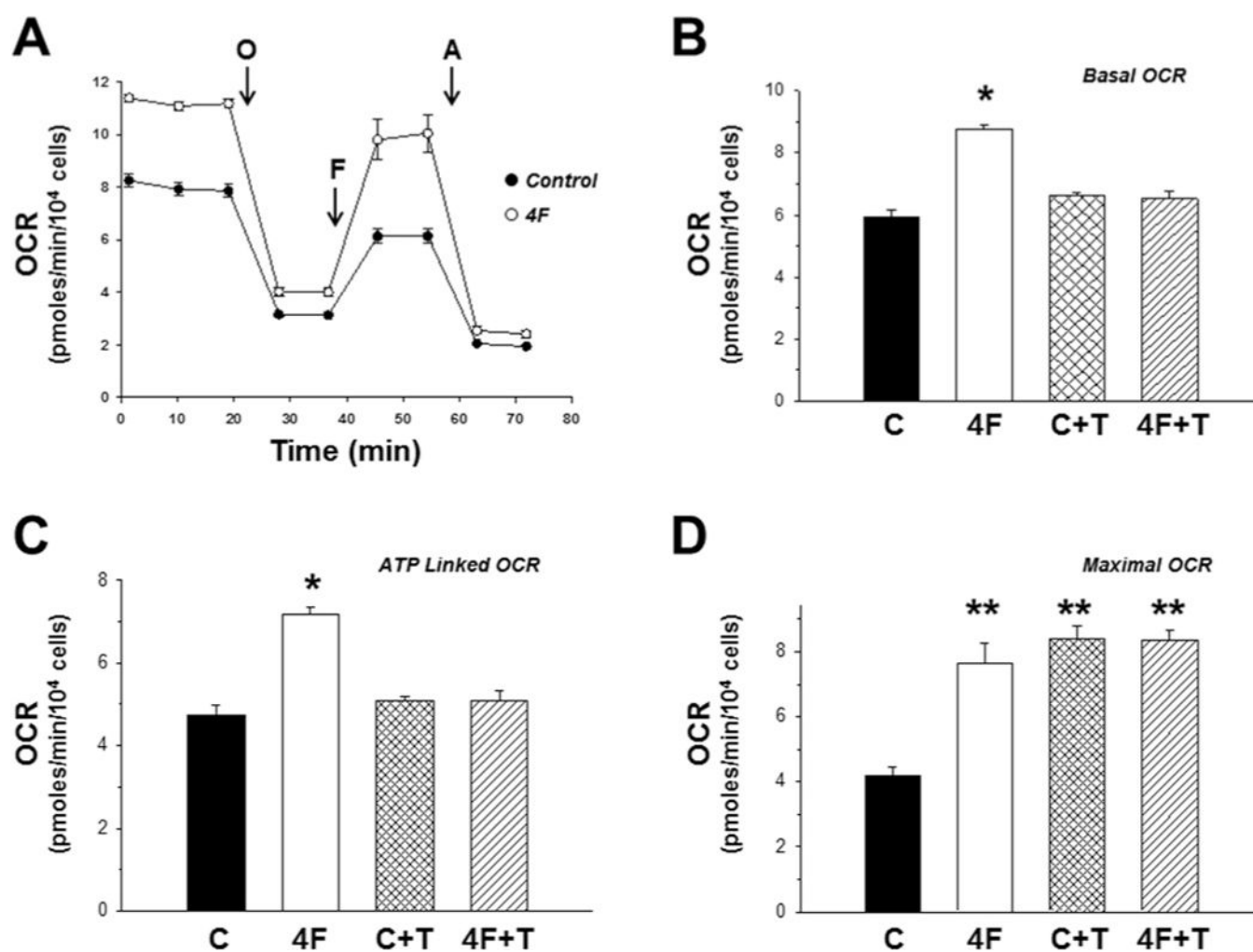


Figure 4. 4F increases mitochondrial oxygen consumption in MDMs

(A) Representative Seahorse profiles of OCR in control (C) and 4F-treated (4F) MDMs. Indices of mitochondrial function were measured by sequential addition of oligomycin (O), FCCP (F) and antimycin A (A), as described in the Experimental section. (B) Basal, (C) ATP-linked and (D) maximal OCR were also calculated. In some experiments, the PPAR γ antagonist T0070907 (T) was added to control and 4F-treated MDMs 24 h before assay. Results are means \pm S.E.M. for five or six replicate wells. * P < 0.05 compared with all other treatment groups. ** P < 0.05 compared with control.

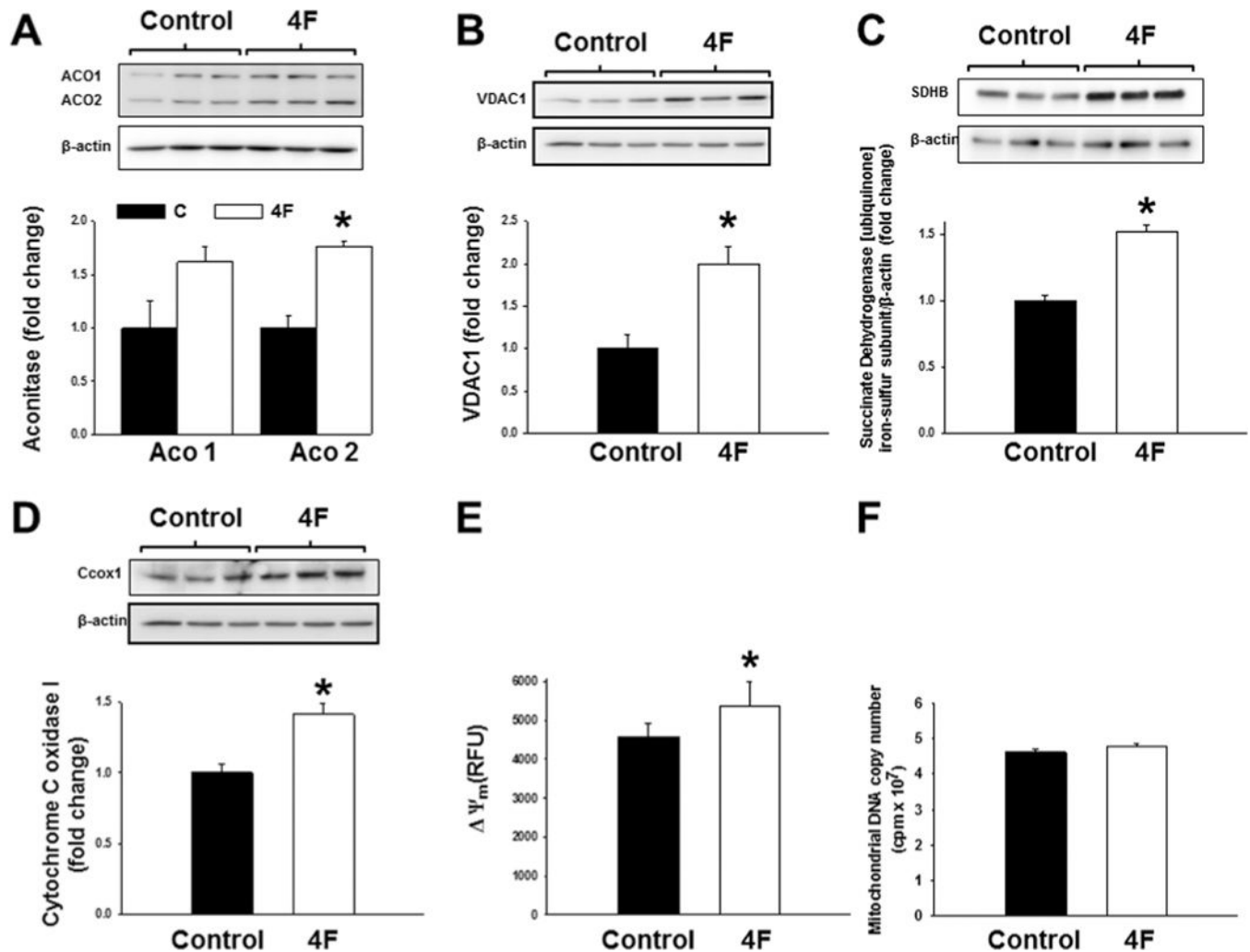


Figure 5. 4F treatment up-regulates mitochondrial proteins and increases Ψ_m in MDMs (A–D) Protein expression for aconitase 1 and 2 (ACO1/ACO2), VDAC1, succinate dehydrogenase (ubiquinone) iron–sulfur subunit (SDHB/Complex II) and cytochrome *c* oxidase I (Ccox1/Complex IV) was measured by densitometry in control (black bar) and 4F-treated (white bar) MDMs. Results are mean \pm S.E.M. fold changes in protein expression compared with control ($n = 3$). (E) Ψ_m was measured using the fluorescent indicator TMRM. Control and 4F-treated MDMs (both $n = 6$) were incubated with TMRM (100 nM) for 30 min at 37°C. Fluorescence emission was monitored at 573 nm using a plate reader (RFU, relative fluorescence units). (F) Mitochondrial DNA copy number was determined by performing a human mitochondrial short PCR. Duplicate samples from control and 4F-treated MDMs were amplified and resolved on a 10% polyacrylamide gel. Dried gels were imaged using a Storm scanner, followed by quantification of DNA product bands. Results are means \pm S.E.M. ($n = 3$). * $P < 0.05$ compared with control.

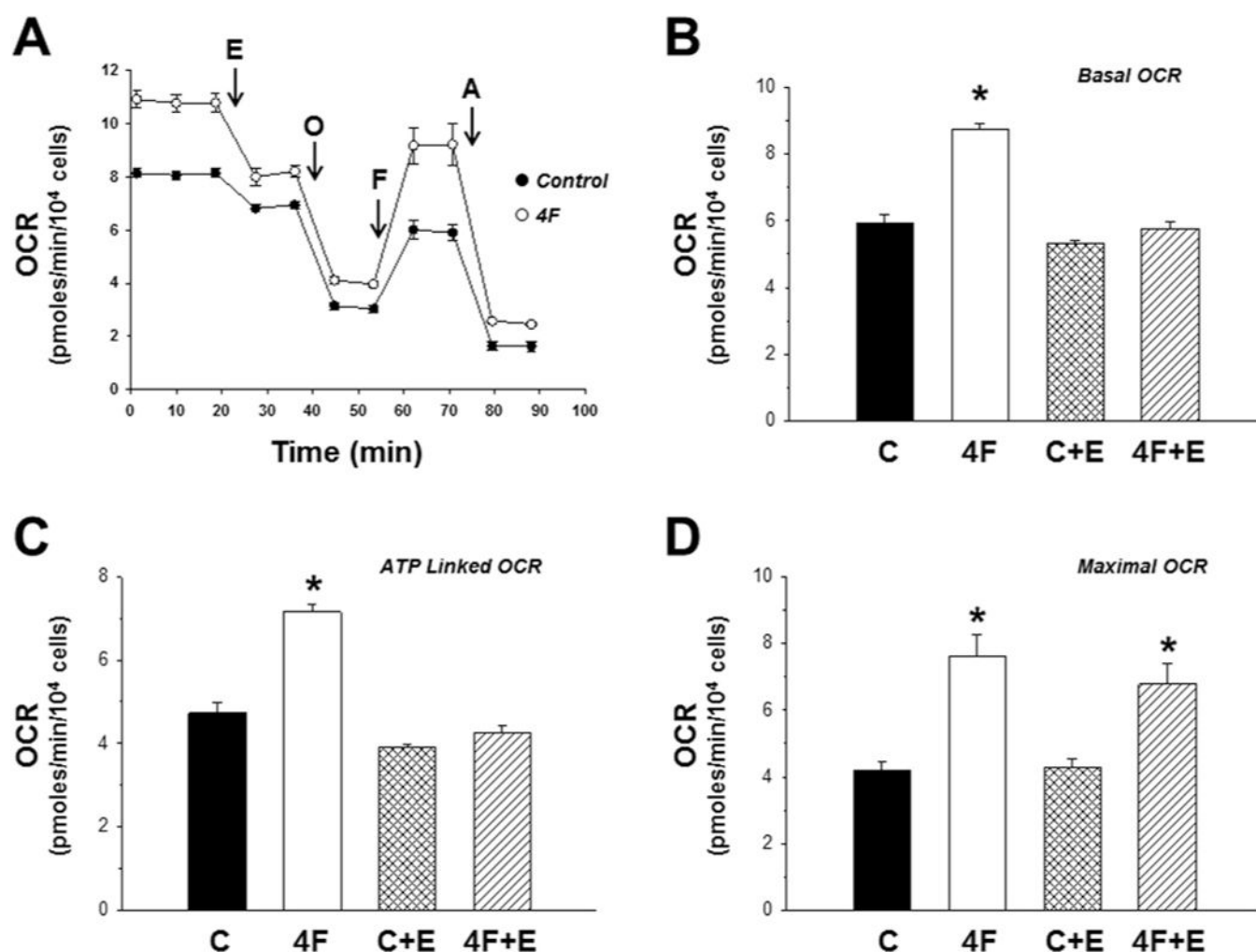


Figure 6. Inhibition of FA uptake attenuates the 4F-mediated increase in mitochondrial oxygen consumption in MDMs

(A) Representative Seahorse profiles of OCR in control and 4F-treated MDMs. Basal OCR was measured, followed by addition of 50 μ M etomoxir (E), an inhibitor of FA uptake. Effects of etomoxir on indices of mitochondrial function were then measured by sequential addition of oligomycin (O), FCCP (F) and antimycin A (A). (B) Basal, (C) ATP-linked and (D) maximal OCR were also calculated. Results are means \pm S.E.M. for three to six replicate wells. * $P < 0.05$ compared with control.

Table 1

Gene-specific primers used in qRT-PCR experiments

Gene	Forward (5'→3')	Reverse (5'→3')
<i>PPAR</i>	GAGAGATCCACGGAGCTGAT	AGGCCATTTTGTCAAACGAG
<i>PPARGC1B</i>	GAGTCAAAGTCGCTGGCATC	AACTATCTCGCTGACACGCA
<i>LPL</i>	TGCAGTTCCAAGGAAGCCTTT	TTGTTGCAGCGGTTCTTCTAC
<i>CD36</i>	CTGTCATTGGTGCTGTCCTG	TGTACCTTCTTCGAGGACAAC
<i>FABP4</i>	GCGTCATGAAAGGCGTCACT	GTCAACGTCCCTTGGCTTATG
<i>FABP5</i>	GCTGATGGCAGAAAACTCAGA	CCTGATGCTGAACCAATGCA
<i>VDAC1</i>	AGGCACCGAGATTACTGTGG	GTTAATGTGCTCCCGCTTGT
<i>RPL37A</i>	CAGTCTTCTGATGGCGGACT	GATCTGGCACTGTGGTTCCT

RPL37A served as a housekeeping gene

Table 2

4F up-regulates genes of lipid metabolism in MDMs

Gene	Entrez gene ID	Entrez gene name	Fold change	S.D.	P-value	q-value
<i>ACAA1</i>	30	Acetyl-CoA acyltransferase 1	+1.4	0.065	1.3×10^{-4}	4.8×10^{-4}
<i>ACAA2</i>	10449	Acetyl-CoA acyltransferase 2	+1.4	0.053	0.001	0.002
<i>ACAT1</i>	38	Acetyl-CoA acetyltransferase 1	+1.6	0.094	1.5×10^{-7}	4.6×10^{-6}
<i>ACAT2</i>	39	Acetyl-CoA acetyltransferase 2	+4.0	0.058	2.6×10^{-8}	1.4×10^{-6}
<i>FABP3</i>	2170	Fatty-acid-binding protein 3	+1.8	0.089	2.5×10^{-9}	2.7×10^{-7}
<i>FABP4</i>	2167	Fatty-acid-binding protein 4	+6.6	0.413	1×10^{-6}	1.7×10^{-5}
<i>FABP5</i>	2171	Fatty-acid-binding protein 5	+5.7	0.174	1.4×10^{-9}	1.8×10^{-7}
<i>CPT2</i>	1376	Camitine palmitoyltransferase 2	+1.3	0.141	3.3×10^{-5}	1.9×10^{-4}
<i>LPL</i>	4023	Lipoprotein lipase	+10.4	0.097	6.1×10^{-5}	2.9×10^{-4}
<i>CD36</i>	948	CD36	+2.7	0.185	2.5×10^{-7}	6.5×10^{-6}
<i>LDLR</i>	3949	Low-density lipoprotein receptor	+2.7	0.105	2.3×10^{-9}	2.6×10^{-7}
<i>PPARG</i>	5468	Peroxisome-proliferator-activated receptor γ	+2.8	0.110	4.4×10^{-6}	4.7×10^{-5}
<i>PPARGC1B</i>	133522	Peroxisome-proliferator-activated receptor γ ; co-activator 1 β	+1.3	0.086	0.00856	0.013
<i>NRIH3</i>	10062	LXR nuclear receptor subfamily 1, group H, member 3	+2.2	0.091	0.0026	0.004
<i>ATF3</i>	467	Activating transcription factor 3	+1.64	0.059	4.07×10^{-4}	0.001

Results are fold changes in gene expression compared with vehicle treatment compiled from four experiments.

Table 3

Effects of 4F on mRNA expression for selected genes in the microarray

Gene	Fold change (4F compared with control)	P-value
<i>PPA R</i>	7.21 ± 1.55	0.002*
<i>PPARGC1B</i>	1.03 ± 0.27	0.900
<i>LPL</i>	4.13 ± 2.28	0.082
<i>CD36</i>	1.63 ± 0.49	0.129
<i>FABP4</i>	66.9 ± 32.0	0.023*
<i>FABP5</i>	12.9 ± 6.56	0.034*
<i>VDAC1</i>	1.51 ± 0.27	0.032*

Results are fold changes in gene expression compared with vehicle treatment compiled from four experiments.

* $P < 0.05$ compared with control.

Table 4

4F up-regulates mitochondrial genes in MDMs

Gene	Entrez gene ID	Entrez gene name	Fold change	S.D.	P-value	q-value
<i>ACADM</i>	34	Acyl-Coenzyme A dehydrogenase	+2.2	0.073	5.8×10^{-7}	1.2×10^{-5}
<i>ACO1</i>	48	Aconitase 1	+1.7	0.080	2.1×10^{-6}	2.8×10^{-5}
<i>ACO2</i>	50	Aconitase 2	+2.1	0.037	0.0027	0.0051
<i>ACOX1</i>	51	Acyl-CoA oxidase 1	+1.2	0.123	1.3×10^{-4}	4.9×10^{-4}
<i>COX5B</i>	1329	Cytochrome <i>c</i> oxidase subunit Vb	+2.1	0.083	0.039	0.049
<i>COX7B</i>	1349	Cytochrome <i>c</i> oxidase subunit VIIb	+2.4	0.12	6.3×10^{-6}	5.9×10^{-5}
<i>NDUFB1</i>	4706	NADH dehydrogenase (ubiquinone) 1 α/β subcomplex 1, 8 kDa	+2.4	0.02	1.5×10^{-8}	9×10^{-7}
<i>NDUFB5</i>	4711	NADH dehydrogenase (ubiquinone) 1 β subcomplex 5, 16 kDa	+2.3	0.031	1.7×10^{-5}	1.1×10^{-4}
<i>NDUFB6</i>	4712	NADH dehydrogenase (ubiquinone) 1 β subcomplex 6, 17 kDa	+2.3	0.029	1.4×10^{-5}	1×10^{-4}
<i>NDUFS1</i>	4719	NADH dehydrogenase (ubiquinone) iron-sulfur protein 1, 75 kDa (NADH-coenzyme Q reductase)	+1.8	0.109	7.7×10^{-5}	3.4×10^{-4}
<i>NDUFS6</i>	4726	NADH dehydrogenase (ubiquinone) iron-sulfur protein 6, 13 kDa (NADH-coenzyme Q reductase)	+1.2	0.032	7.6×10^{-7}	1.4×10^{-5}
<i>SDHB</i>	6390	Succinate dehydrogenase complex, subunit B	+1.4	0.097	7.6×10^{-6}	6.8×10^{-5}
<i>SDHC</i>	6391	Succinate dehydrogenase complex, subunit C	+1.7	0.132	2.6×10^{-5}	1.6×10^{-4}
<i>SDHD</i>	6392	Succinate dehydrogenase complex, subunit D	+1.4	0.139	0.003	0.006
<i>SOD1</i>	6647	Superoxide dismutase 1	+1.2	0.035	3.6×10^{-7}	8.4×10^{-6}
<i>VDAC1</i>	7416	Voltage-dependent anion channel 1	+1.6	0.122	4.0×10^{-4}	0.001
<i>VDAC2</i>	7417	Voltage-dependent anion channel 2	+1.3	0.171	0.006	0.01
<i>VDAC3</i>	7419	Voltage-dependent anion channel 3	+1.5	0.049	4.6×10^{-5}	2.4×10^{-4}

Results are fold changes in gene expression compared with vehicle treatment compiled from four experiments.